Journal of Organometallic Chemistry 996 (2023) 122743

Contents lists available at ScienceDirect

Journal of Organometallic Chemistry

journal homepage: www.elsevier.com/locate/jorganchem

Tandem Heck/Tsuji-Trost Reaction for Uncaging of Alloc-Protected Amines with Palladium Complexes in Living Cells

Yonghua Tan[a,b], Marine Lefevre[a,c], François Pierrard[a,b], Mathieu Soetens[a], Maria Shoueiry[a], Esra Yildiz[b], Sébastien Ibanez[c], Kubra Ozkan[c], Olivier Feron[c], Raphaël Frédérick[b,*], Olivier Riant[a,*]

[a] Institute of Condensed Matter and Nanosciences (IMCN), Université catholique de Louvain, Louvain-la-Neuve 1348, Belgium
[b] Louvain Drug Research Institute (LDRI), Université catholique de Louvain, Brussels B-1200, Belgium
[c] Pole of Pharmacology and Therapeutics (FATH), Institut de Recherche Expérimentale et Clinique (IREC), Université catholique de Louvain, Brussels B-1200, Belgium

ARTICLE INFO

Article history:
Received 20 December 2022
Revised 2 May 2023
Accepted 3 May 2023
Available online 5 May 2023

Keywords:
Palladium
Bioorthogonal chemistry
Reaction mechanism
Fluorescence
Kinetics

ABSTRACT

The palladium-catalyzed uncaging of alloc-protected amines in living cells has been extensively studied mostly in the form of nanostructures or mesostructures. However, the scarcity of kinetic and mechanistic studies of discrete palladium complexes for deallylation reactions has hindered progress. Herein, we report the development of a series of discrete palladium complexes bearing acetanilide ligands, which exhibit a good balance between reactivity and stability in living cells. We investigated the catalytic activity and cytotoxicity of these complexes in SiHa cells and found that acetanilide[tri(2-furyl)phosphine]palladium(II) triflate showed promising results. Under physiological conditions, this palladium complex exhibited a second-order reaction rate of 30 M^{-1} s^{-1}, and liquid chromatography-mass spectrometry (LC-MS) studies suggested the possibility of a tandem Heck/Tsuji-Trost mechanism. Our results demonstrate the potential of using these discrete palladium complexes for bioorthogonal chemistry studies in living cells.

1. Introduction

From the 2008 Nobel Prize for genetically encoded fluorescent protein to the 2022 Nobel Prize for bioorthogonal chemistry, chemists and biologists have always paid interest in developing chemical methodologies compatible with living settings [1,2]. Organometallics are increasingly gaining attention as tools in this bioorthogonal chemistry field [3–10]. Designing metal catalysts that work under physiological conditions is a significant challenge owing to the presence of air, water, and a plethora of chemical functionalities *in cellulo* [11,12]. It has been reported that discrete, biocompatible, small abiotic metal complexes can cross cell membranes and promote new-to-nature intracellular transformations [13–16]. The first evidence of bioorthogonal catalysis was reported in 2006 by Meggers and co-workers. They developed ruthenium complexes capable of mediating the uncaging of allyloxycarbonyl (alloc)-protected amines in living mammalian cells [19–22]. Since then, chemical biologists have focused on expanding the scope of metal-catalyzed biocompatible reactions.

Among widely studied metals in catalysis, palladium is very appealing because of its well-demonstrated versatility in catalytic cross-coupling reactions thereby opening new opportunities for biolabeling or drug delivery [17–21]. However, most applications reported so far involve the use of Pd nanostructures or mesostructures, rather than discrete complexes, to alleviate potential stability issues. In 2011, Bradley reported that palladium nanoparticles within polystyrene microspheres cleaved allyl carbamate groups in HeLa cells (Scheme 1a) [22]. The same group also developed cancer-targeting palladium nanoparticles for the activation of prodrugs, 5-fluorouracil, and cytotoxic agent PP121 simultaneously [23–25]. Later, Weissleder and co-workers envisioned cleaving the allyloxycarbonyl group with discrete bis[*tri*(2-*furyl*)*phosphine*]palladium(II) dichloride complex ($PdCl_2(TFP)_2$) but they encountered solubility and stability issues. This problem was solved by encapsulating the complex in a biocompatible poly(lactic-*co*-glycolic acid)-polyethyleneglycol (PLGA-PEG) nanoparticle (Scheme 1b) [26]. Two more examples were developed by Unciti-Broceta with Pd^0-resin and Chen with Pd nanoparticles to promote depropargylation reactions in living settings (Scheme 1c) [27,28]. Nevertheless, the use of discrete palladium complexes remains attractive because of their defined struc-

* Corresponding authors.
E-mail address: olivier.riant@uclouvain.be (O. Riant).

https://doi.org/10.1016/j.jorganchem.2023.122743
0022-328X/

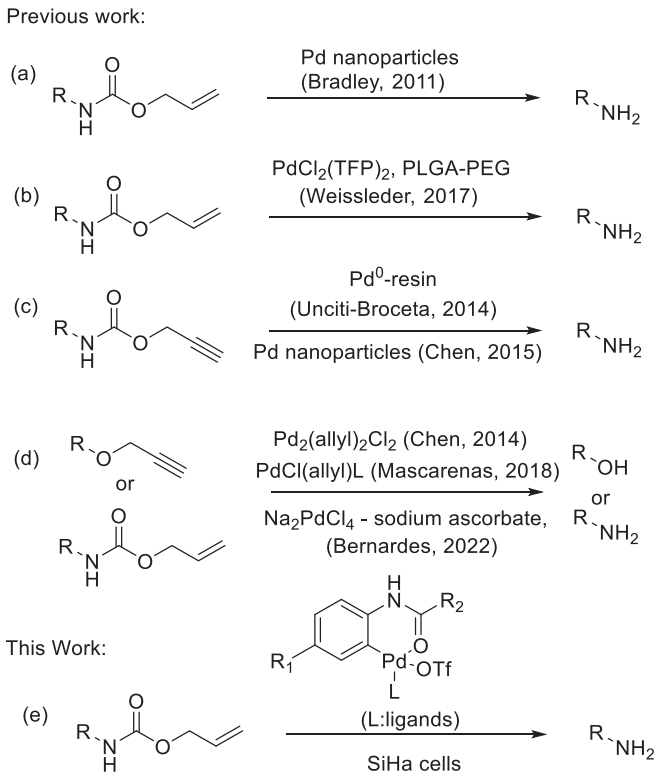

Scheme 1. (a) Bradley: deallylation reactions mediated by Pd nanoparticles in microspheres; (b) Weissleder: Pd^{II} complexes in biodegradable nanoencapsules; (c) Unciti-Broceta and Chen: depropargylation reactions catalyzed by Pd^0-resin or Pd nanoparticles; (d) Chen, Mascarenas, and Bernardes: uncaging of propargyl-protected alcohols and alloc-protected amines catalyzed by discrete palladium complexes; (e) This work: uncaging reaction catalyzed by discrete palladium complexes bearing acetanilide functionalities.

ture and the possibility to manipulate their ligands to fine-tune their solubility, stability, toxicity, and reactivity properties or even favor cell transport and intracellular targeting [29]. Such biocompatible complexes have also been described, but more sporadically. Chen's group showed that $Pd_2(allyl)_2Cl_2$ can cleave propargyl and allocgroups in phosphate buffered saline (PBS) at 37 °C and in HeLa cells (Scheme 1d). Furthermore, they discovered that $Pd_2(allyl)_2Cl_2$ and $Pd(dba)_2$ decaged an allene-based moiety [30,31]. In addition, Mascarenas used discrete palladium complexes with newly designed mitochondria-targeting phosphine ligands to cleave propargyl and alloc groups in 2018 (Scheme 1d). They observed that labile phosphine ligands were not the most reactive but showed better resistance to hostile media thereby enhancing the complexes' stability [26,32]. Furthermore, Bradley's group designed a palladium complex conjugated to a cell-penetrating peptide [33]. These examples illustrate the importance of ligand engineering to enhance biocompatibility and simplify the catalyst preparation process.

As demonstrated in several works, bond-cleavage reactions can successfully occur in living systems but there is no clear understanding of the mechanism involved in these reactions. Most examples involve the use of inactive Pd^{II} while it has to be reduced into Pd^0 to perform cross-coupling reactions. In 2013, Wei and co-workers proposed two base-promoted pathways for the in situ generations of Pd^0L_n (n = 1 or 2). One of the pathways was phosphine-mediated reduction whereas the other was diboron-mediated [34]. Recently, Bernardes' group utilized Na_2PdCl_4 as the precursor to deliver active Pd^0 species following sodium ascorbate reduction inside living cells (Scheme 1d) [35]. In brief, the development of discrete palladium complexes with novel ligands and further investigation of the reaction mechanism under biological conditions will provide a basis for a wide application in bioorthogonal chemistry.

In this study, we report the development and evaluation of a series of acetanilide palladium complexes for use in bioorthogonal catalysis. These discrete, biocompatible complexes have been designed to promote deallylation reactions in living mammalian cells, and their efficiency and mechanism of action have been investigated through LC-MS studies. Our results demonstrate the potential of these palladium complexes as effective tools for bioorthogonal chemistry and highlight the importance of ligand engineering in the development of biocompatible catalysts for use in living systems.

2. Materials and methods

2.1. Chemical section

2.1.1. Generalities

Unless otherwise specified, all reactions were conducted in air at room temperature. The solvents used for the workup were of technical grade without distillation. Commercial reagents were purchased from Acros, Sigma-Aldrich, TCI, and Fluorochem and used without purification unless stated otherwise. High-resolution mass spectra were obtained from a Thermo Scientific QExactive mass spectrometer, with accurate mass reported for either the molecular ion or suitable fragment ions. ESI-LC/MS spectra were obtained using an Agilent (1100 series) HPLC single quadrupole (InfinityLab, ESI+) system equipped with a ZORBAX SB-C18 5 μm (150 mm × 4,6 mm).

2.1.2. General synthetic procedure for the palladium complexes

Palladacycles were prepared according to analogous reported methods [36]. A 25 mL flask was equipped with a magnetic stir bar and filled with acetanilide (0.445 mmol), $Pd(OAc)_2$ (100 mg, 0.445 mmol), and 1,4-dioxane (5 mL). After 5 min of stirring at room temperature the acid (0.445 mmol) was added. The mixture was stirred at room temperature for 15 h. The reaction medium was then filtered and washed with hexane before being dried to obtain the desired palladacyclic dimer. The ligand (0.2 mmol) was subsequently added into a THF (1 mL) solution of the previous palladacyclic dimer (0.1 mmol) under nitrogen. The resulting mixture was stirred at room temperature until the reaction was completed, as indicated by ^{31}P NMR spectroscopy. When the product precipitated from the solution, 2 mL of hexane was added. The resulting precipitate was filtered, then rinsed with hexane, collected, and dried to afford the desired monoligated palladacyclic compound. When the product did not precipitate from the solution, the solvent was evaporated under reduced pressure. The resulting residue was triturated with hexane, filtered, washed, and dried to afford the desired compound.

2.1.3. General method for LC-MS experiments

LC-MS analysis was performed using an Agilent (1100 series) LC–MS single quadrupole (InfinityLab ESI+) system equipped with a ZORBAX SB-C18 × 5 μm (150 mm × 4.6 mm), using a distilled water + 0.1% TFA (buffer A) and acetonitrile + 0.1% TFA (buffer B) gradient. Initial conditions for routine analysis were 5% B + 95% A at a flow rate of 1 mL/min, followed by an increase of solution B to 65% in 12 min.

2.1.4. General procedure for catalytic deprotection of RhoMA *in vitro*

The catalytic deprotection of allyloxymorpholinecarbonyl-rhodamine 110 (RhoMA, Fig. 2) to morpholinecarbonyl-rhodamine

110 (RhoM, Fig. 2) under biologically relevant conditions was performed in an translucent 96-well microplates (Microtest 96, BD Falcon). A solution of RhoMA (0.5 µL, 1.6 M in DMSO, 1.0 equiv) and a solution of TFP (1 µL, 0 M, 0.4 M, 0.8 M, 1.6 M, 3.2 M, or 8 M in DMSO, from 0 to 10 equiv) were added to phosphate buffer (198 µL, 10 mM, pH 8). After mixing, a solution of the catalyst (0.5 µL, one of concentration 0.08 M, 0.16 M, 0.32 M, 0.6 M, 1 M, 1.2 M or 1.6 M in DMSO, from 0 to 1.0 equiv) was added. The reaction mixture was mixed again. Every 15 min, the reaction mixture was analyzed in a microplate reader (Molecular Devices, LLC, Sunnyvale, CA) at 37 °C. The fluorescence of each well was measured at λ_{ex} = 490 nm, λ_{em} = 520 nm.

2.2. Biology section

2.2.1. Generalities

General Executions and Substances: all steps were performed on a sterile clean bench (ESCO Laminar Flow Cabinet) at room temperature. Solutions stored in a fridge were warmed beforehand in a water bath (37 °C). All substances were supplied by Sigma-Aldrich.

Cell Culture: SiHa cells were cultured in a T75 flask (Greiner bio-one) with DMEM (Gibco) supplemented with fetal bovine serum (FBS; 10 vol%), penicillin (100 U/mL) and streptomycin (0.1 mg/mL). The cells were incubated at 37 °C in a 5% CO_2 atmosphere (Excella ECO-170 CO_2 Incubator) and were passaged after 2–3 days before they reached confluence.

Kinetic measurements: the Fluorescence intensity was recorded at 37 °C on a Spectramax® M2E spectrophotometer (Molecular Devices, LLC, Sunnyvale, CA) in 96-well plates.

2.2.2. General procedure for cell viability assays

Cytotoxicity of complexes **Pd1**-**2** and **Pd10**-**15** was evaluated by PrestoBlue assays in SiHa cells as follows: ~10.000 SiHa cells were seeded in translucent 96-well microplates (Microtest 96, BD Falcon) with 100 μL Dulbecco's Modified Eagle Medium (DMEM). After 30 h of incubation, 50 µM RhoMA, TFP (various concentration) (20 µM palladium complexes with 1% DMSO in DMEM (100 μL) were added. Negative control cells were treated with 1% DMSO in DMEM (100 μL). Wells containing corresponding compounds without cells were used as blanks. After 24 h (TFP) or 18 h (RhoMA, RhoM, palladium complexes, and $PdCl_2(TFP)_2$) of incubation, DMEM was removed and a solution of 10% PrestoBlue in DMEM was added. After 0.5 h of incubation at 37 °C, the fluorescence of each well (proportional to the number of living cells) was recorded at λ_{ex}=560 nm, λ_{em}=590 nm using a microplate reader (Molecular Devices, LLC, Sunnyvale, CA). The SD error bar of three independent experiments was shown and curves were compiled using GraphPad software.

2.2.3. General procedure for catalytic reaction in SiHa cells

SiHa cells were seeded in translucent 96-well microplates (Microtest 96, BD Falcon) at ~10.000 cells/well, with 100 µL of DMEM, and incubated for 30 h. Then, 50 µM RhoMA was added and the plates were incubated for an additional 18 h before being rinsed three times with PBS. Palladium complexes (100 µL, 40 µM in DMEM with 1% DMSO) and TFP (100 µL, 80 µM in DMEM with 1% DMSO) were added to the wells. Negative control cells were treated with 1% DMSO in DMEM. Wells containing only culture medium were used as blanks. The fluorescence of each well was measured at λ_{ex} = 490 nm, λ_{em} = 520 nm using a microplate reader (Molecular Devices, LLC, Sunnyvale, CA). Every independent experiment was performed in triplicate on the plate. The SD error bar of three independent experiments was shown and curves were compiled using GraphPad software.

2.2.4. General procedure for live-cell imaging

The catalytic deprotection of RhoMA to RhoM within SiHa cells was studied using confocal fluorescence imaging (LSM800, Zeiss). SiHa cells were adjusted to a concentration of 15.000 cells/well, seeded with DMEM (300 µL) on imaging dishes (NuncTM Lab-TekTM II 8-well chambered cover glass), and incubated for 24 h. The dish was filled with a solution of caged RhoMA (1.5 µL, 100 mM in DMSO) and DMSO (1.5 µL). The dish was incubated at 37 °C for 30 min. Subsequently, the medium was removed, the cells were washed with PBS (2 × 300 µL) and then a solution of fresh DMEM (300 µL) with a solution of catalyst **Pd1** or **Pd2** (1.5 µL, 4 mM in DMSO) and TFP (1.5 µL, 8 mM in DMSO) were added. The cells were incubated at 37 °C and 5% CO_2 during the imaging process. The green fluorescence from free RhoM (λ_{ex} = 488 nm, λ_{em} = 500–650 nm) was used to measure catalytic deprotection. The cells were detected with Hoechst 33342 (λ_{ex} = 405 nm, λ_{ex} = 410–500 nm) as a negative control. The software Zen was used for image capture and processing.

3. Results and discussion

3.1. Design of a library palladium complexes with potential for bioorthogonal chemistry studies

Air- and moisture-stable monodentate or bidentate aryl palladacyclic complexes containing acetanilide functionalities (Fig. 1) were synthesized from simple, inexpensive starting materials to investigate their potential for bioorthogonal chemistry [39,41,42]. Our library aimed to establish structure-activity relationships by investigating the influence of bidentate or monodentate ligands coordinated to the palladium center (**Pd1**–**9**), the anionic ligand (**Pd10**–**12**), and the nature of the substituent on the acetanilide core (**Pd13**–**15**). Although some of these complexes have previously been demonstrated to catalyze cross-coupling reactions [39], to the best of our knowledge, their potential for Tsuji-Trost deallylation under physiological conditions has not been explored.

3.2. Optimization of Pd-catalyzed deallylation reaction in aqueous solution

To evaluate the potential of the synthesized palladium complexes for bioorthogonal chemistry studies, we investigated their ability to promote the deallylation reaction under physiological conditions. Specifically, we focused on acetanilide[*tri*(2-*furyl*)*phosphine*]palladium(II) triflate (**Pd1**), which showed promising results in preliminary studies.

In order to optimize the deallylation reaction, we conduced a fluorogenic model reaction using NcoumAlloc as the substrate (Table 1). Our initial study revealed that **Pd1** was able to cleave the non-fluorescent NcoumAlloc probe, yielding the fluorescent compound **1a**. However, the ON/OFF ratio between NcoumAlloc and **1a** was low, and the emission spectra of NcoumAlloc and **1a** showed significant overlap, making it difficult to perform kinetic measurements and further screening of the complexes (Fig. S1). Hence, we employed LC-MS to conduct preliminary evaluations (Table 1).

In our initial experiment (entry 1, Table 1), we conducted a reaction between equimolar amounts of NcoumAlloc and **Pd1** in water at 37 °C, which resulted in a modest 12% yield of product **1a**. To improve the yield of **1a**, we screened phosphate buffers at different pH values and found basic conditions pH 9 to be more favorable (entries 2–5, Table 1). However, a considerable amount of byproduct **1b** was generated in each experiment, likely due to the lack of efficient nucleophiles for π-allylpalladium intermediate capture (see Section 3.6).

Consistently, the team of Meggers reported that a similar byproduct was not observed in the presence of an excess of nu-

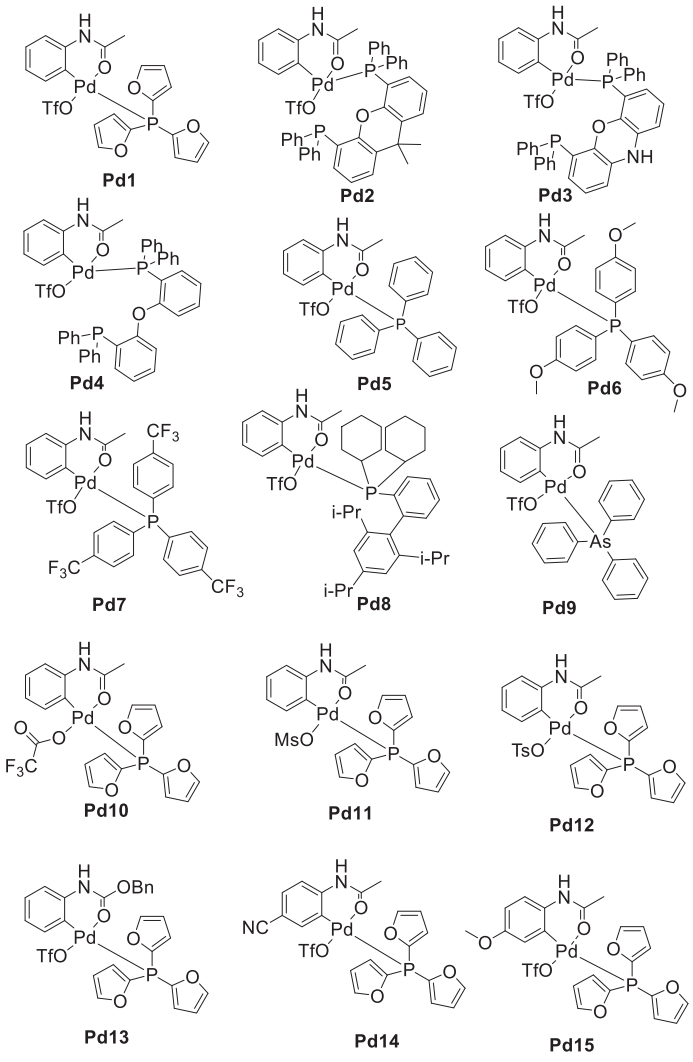

Fig. 1. Structure of the Pd catalysts used in this work.

cleophiles such as glutathione. Colacot *et al.* reported that triethylamine (TEA) could be used as a base for Pd^{II} activation into Pd^0 [38]. We speculated that triethylamine (TEA) could play a dual role as a nucleophile and an activator of Pd^{II} into Pd^0. We tested different amounts of TEA and found that increasing its amount to 95 equivalents resulted in a complete reaction and no detection of byproduct (Fig. S4). Moreover, a yield of 50% was achieved in only 5 min (Fig. S5). When only 0.1 equivalent of **Pd1** was used, a yield of 62% was obtained after 30 min, with a turnover number (TON) of 6.2 and a turnover frequency (TOF) of 12.4 h^{-1} (entry 8, Table 1). Control experiments showed no spontaneous degradation of NcoumAlloc under these conditions (Fig. S6).

3.3. Investigating the structure-activity relationship of palladium complexes

The catalytic activity of our series of palladium complexes for the deallylation of allyl-protected amines in water was evaluated to establish a structure-activity relationship. After the reaction under the optimized conditions (entry 7, Table 1), LC-MS analysis showed that all of the palladium complexes were able to promote the deallylation reaction to some extent, with yields ranging from 2% to 98% (Table 2).

Firstly, our results indicated that the choice of phosphine ligand plays a crucial role in determining the catalytic activity of the complex. The bidentate phosphine ligands examined in this study, including Xantphos (**Pd2**), N-Xantphos (**Pd3**), and DPEphos (**Pd4**), showed varying yields of 84%, 17%, and 23%, respectively. This disparity could be attributed to the different bite angles imposed by each ligand on the respective complex (Xantphos = 108^0, N-Xantphos = 114^0, DPEphos = 104^0). The catalyst that exhibited the highest activity, Xantphos (Pd2), had an angle close to 110°, which is an optimal value already reported in the literature for deallylation reactions [13–15]. However, TFP (**Pd1**) showed the most attractive properties with a yield of 98%, while other monodentate ligands presented a low yield around or below 25% (Table 2, entries 5-7). Indeed, TFP is known to facilitate dissociation from the metal, leaving d-orbitals available for oxidative addition and promoting nucleophilic turnover of the π-allylpalladium species, and stabilizing Pd^0 species generates in situ [39].

Secondly, the introduction of different acid groups as the anionic ligand to the palladium complexes, such as trifluoroacetate (**Pd10**), mesylate (**Pd11**), and tosylate (**Pd12**), led to high efficiency comparable to **Pd1** thereby showing no considerable influence on the catalytical activity.

Finally, the replacement of the acetamido group in **Pd1** by a benzyl carbamate (**Pd13**) decreased the deallylation efficiency

Table 1
Pd-catalyzed deallylation reaction optimization.

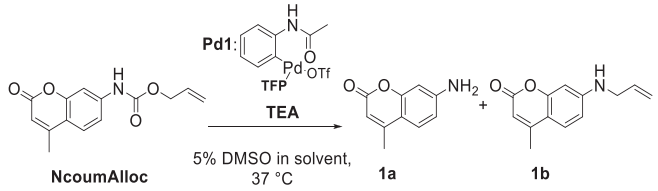

Entry	Conditions[a]				Yield[b]	
	NcoumAlloc (mM)	**Pd1** (mM)	TEA (mM)	Solvent	**1a** (%)	**1b** (%)
1	0.1	0.1	0	H_2O	12[d]	2
2	0.1	0.1	0	pH 6.0[c]	19[d]	2
3	0.1	0.1	0	pH 7.4 [c]	54[d]	3
4	0.1	0.1	0	pH 8.0 [c]	61[d]	2
5	0.1	0.1	0	pH 9.0 [c]	66[d]	3
6	0.1	0.1	1	H_2O	20[e]	0
7	0.1	0.1	9.5	H_2O	98[e]	0
8	0.1	0.01	9.5	H_2O	62[e]	0

[a] Detailed conditions are shown in Table S1.
[b] HPLC yields determined by the calibration curves (Fig. S2 and Fig. S3).
[c] 10 mM potassium phosphate buffer.
[d] Yield obtained after stirring at 37 °C for 12 h.
[e] Yield obtained after stirring at 37 °C for 30 min.

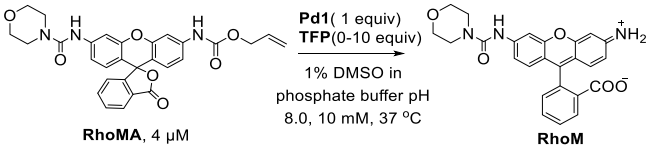

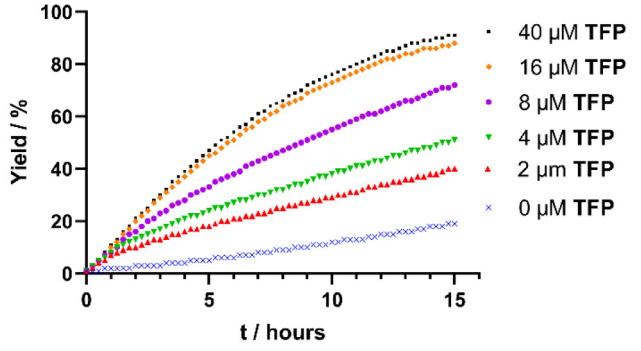

Fig. 2. Evaluation of the effect of TFP on the catalytic activity of palladium complex **Pd1**. Reaction conditions: RhoMA (1.0 equiv, 4 µM), **Pd1** (1 equiv,4 µM), and TFP (0- 40 µM) in 1% DMSO in phosphate buffer 10 mM pH 8.0 at 37 °C. The yield was determined by the fluorescence calibration curve of RhoM (λ_{ex}=490 nm, λ_{em}=520 nm, Fig. S7B).

(Table 2, entry 13) while other modifications with an electron-donating or an electron-withdrawing group (Pd14–15) led to palladium complexes (Table 2, entries 14–15) with similar alloc uncaging capabilities as the reference Pd1. Overall, discrete palladium complexes containing acetanilide functionalities and coordinating TFP (Pd1, Pd10-Pd12) demonstrated excellent deallylation reactivity in water.

In addition, two commercial palladium complexes $Pd(PPh_3)_4$ [40] and $Pd(OAc)_2$ [30] were also studied as control sources of Pd^0 and Pd^{II} respectively (Table 2, entries 16–17). Under the previously optimized conditions, $Pd(PPh_3)_4$ proved to be very efficient while $Pd(OAc)_2$ performed poorly, thereby confirming that the presence

Table 2
Screening of palladium complexes for deallylation reaction in water[a].

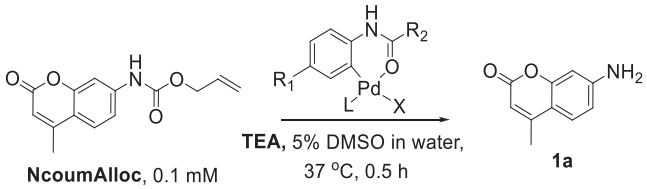

Entry	Name	Pd complexes [b]				Yield (%) [c]
		L	X	R_1	R_2	
1	**Pd1**	TFP	OTf	H	CH_3	98
2	**Pd2**	Xantphos	OTf	H	CH_3	84
3	**Pd3**	*N*-Xantphos	OTf	H	CH_3	17
4	**Pd4**	DPEphos	OTf	H	CH_3	23
5	**Pd5**	PPh_3	OTf	H	CH_3	6
6	**Pd6**	$(p\text{-}CH_3OC_6H_4)_3P$	OTf	H	CH_3	2
7	**Pd7**	$(p\text{-}CF_3C_6H_4)_3P$	OTf	H	CH_3	25
8	**Pd8**	Xphos	OTf	H	CH_3	25
9	**Pd9**	$AsPh_3$	OTf	H	CH_3	18
10	**Pd10**	TFP	CF_3COO	H	CH_3	95
11	**Pd11**	TFP	OMs	H	CH_3	96
12	**Pd12**	TFP	OTs	H	CH_3	98
13	**Pd13**	TFP	OTf	H	OBn	63
14	**Pd14**	TFP	OTf	OCH_3	CH_3	98
15	**Pd15**	TFP	OTf	CN	CH_3	95
16	$Pd(PPh_3)_4$	/	/	/	/	77
17	$Pd(OAc)_2$	/	/	/	/	5

[a] Reaction conditions: NcoumAlloc (0.1 mM), Pd complexes (0.1 mM), TEA (9.5 mM), 5% DMSO in water, 37 °C, 30 min.
[b] Synthesis route and characterization of the palladium complexes are shown in the supporting information.
[c] HPLC yields determined by the calibration curve (Fig. S2).

of Pd^0 and a ligand is essential to perform deallylation reactions in aqueous solutions [39].

3.4. Investigation of the kinetic parameters of Pd1-catalyzed deallylation reaction in physiological conditions

Section 3.2 demonstrated the enhanced catalytic activity of **Pd1** in basic aqueous solutions pH 9, which was established with our coumarin model. However, these conditions are not suitable to evaluate the potential use of the synthesized palladium complexes for bioorthogonal chemistry studies. The studied pH is too far from physiological conditions, and coumarin **1a**, which was used in the previous study, is known to have antiproliferative effects [41].

Therefore, we synthesized another fluorogenic model consisting of a caged form of rhodamine, RhoMA (Fig. 2) previously reported for copper-catalyzed deallylation reactions [42]. RhoMA is nonfluorescent and stable in an aqueous solution and can release the highly fluorescent RhoM upon deallylation with an excellent ON/OFF ratio of 191 (Fig. S7).

The deallylation reaction was initially carried out in phosphate buffer at pH 8.0, using 4 µM RhoMA and 4 µM **Pd1**. But it presented a yield below 20%, even after a long reaction time of 15 h (Fig. 2, light blue curve). By increasing the TFP concentration up to 40 µM, we observed enhanced kinetic release of RhoM with a yield reaching 90% after 15 h of reaction. Moreover, we found that the turnover number (TON) was dependent on the substrate concentration, with the highest TON of 8.0 achieved when 0.05 equivalent of **Pd1** were supplemented with 40 µM of TFP (Fig. S8). Additionally, we measured the second-order rate constant k_2 of **Pd1** at 37 °C, which was found to be 30 M^{-1} s^{-1} (Fig. 3). These results suggest that **Pd1** is an effective catalyst for the deallylation

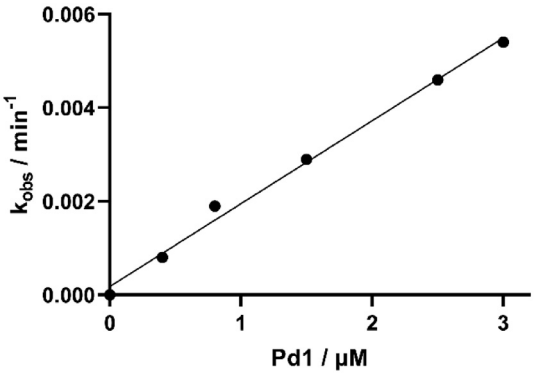

Fig. 3. Evaluating second-order rate constant k_2 = 0.001772 $\mu M^{-1}min^{-1}$ = 30 M^{-1} s^{-1} of **Pd1** in the reaction with RhoMA under biologically relevant conditions. Conditions: RhoMA 4 μM, TFP = 16 μM, 1% DMSO in phosphate buffer 10 mM pH 8.0, 37 ^{0}C, λ_{ex} = 490 nm, λ_{em} = 520 nm (Table S2).

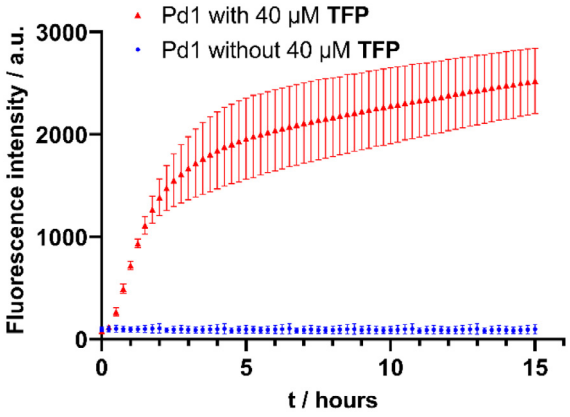

Fig. 4. Evaluation of the effect of TFP on the release of RhoM from RhoMA in SiHa cells Procedure: 50 μM RhoMA incubation for 18 h, then washed with PBS 3 times, 20 μM **Pd1** in fresh culture medium 1% DMSO with TFP or without TFP, Fluorescence intensity was followed for 15 h at 37 °C, λ_{ex}=490 nm, λ_{em}=520 nm. Error bars: ± SD from n = 3.

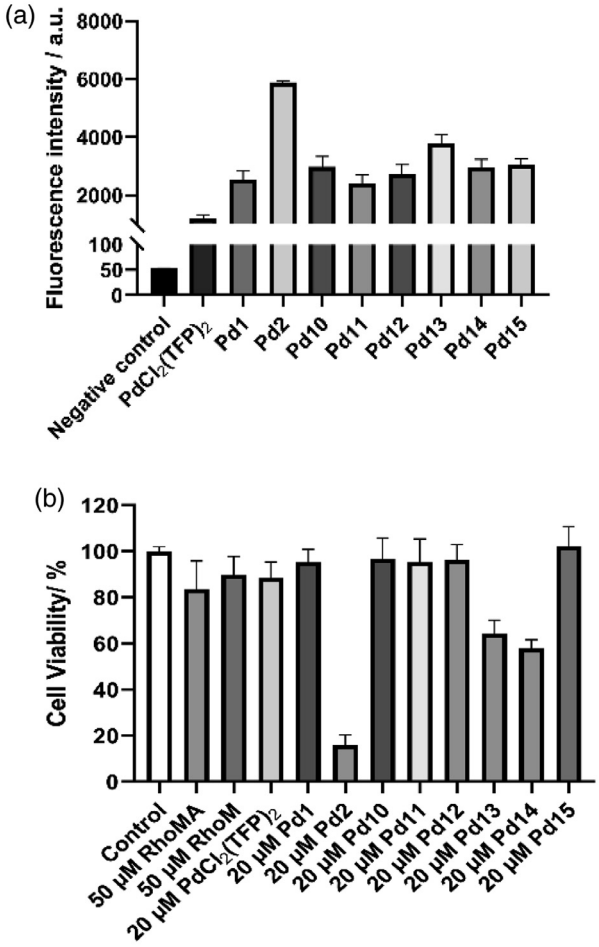

Fig. 5. Discrete palladium complexes catalyzing from RhoMA to RhoM in SiHa cells. (a) Bar diagram representation of fluorescence intensity obtained for each palladium complex after incubation 15 h in SiHa cells. Procedure: RhoMA 50 μM incubation for 18 h, then washing with PBS three times, 20 μM Pd complexes incubated with 40 μM TFP for 15 h, then fluorescence was measured at λ_{ex}=490 nm, λ_{em}=520 nm 37 °C. Error bars: ± SD from n = 3. (b) The evaluation of palladium complexes' cell viability. Conditions: RhoMA (50 μM), RhoM (50 μM), or palladium complexes ($PdCl_2(TFP)_2$, **Pd1**, **Pd2**, **Pd10**-**Pd15**)(20 μM) incubated for 18 h in an incubator, removed the culture medium, then 10% Presto Blue was added and in 37 °C, 5% CO_2 incubation for 30 min, then measure at λ_{ex}=560 nm, λ_{em}=590 nm, Error bars: ±SD from n = 3.

reaction in physiological conditions and that the TFP co-ligand is important for enhancing the reaction kinetics.

3.5. Evaluating the efficacy and cytotoxicity of Pd complexes for the deallylation reaction in living cells

Driven by these encouraging results, we set out to investigate if our palladium catalysts could be used in cell-based settings using SiHa cells as a cellular model, as those cells have been widely used by other groups for the investigation of transition-metal-based catalytic reactions [43]. For each experiment, the cell culture was first incubated with the pro-fluorophore RhoMA for 18 h, to ensure cell penetration. After removing excess RhoMA from the medium, we incubated the culture with the palladium catalyst and recorded fluorescence for 15 h.

In a pilot experiment, we evaluated the deallylation reaction of RhoMA using the **Pd1** complex, both in the absence and presence of TFP. Similar to our in vitro assessment (Section 3.4), we observed poor RhoM release in the absence of TFP, while the addition of 40 μM TFP led to a substantial release of RhoM (Fig. 4). These results supported our earlier conclusion that an excess of TFP is required to stabilize the Pd^0L_n species and promote the bioorthogonal deallylation reaction, even in a cell-based setting. Moreover, we found that TFP exhibited no cytotoxicity (Fig. S12).

Using these conditions, the best palladium complexes from this study (**Pd1**–**2**, **Pd10**–**15**) were evaluated *in cellulo*. They all performed very well in uncaging RhoMA, with fluorescence intensities higher than the reference $PdCl_2(TFP)_2$ (Fig. 5a), previously reported by Weissleider et al. [44]. We could anticipate that this higher efficiency arises from a catalytically active palladium complex $L_2Pd^0(Solvent)_n$ (that would be similar for each complex), compared to the L_2PdCl_2 reference palladium complex which requires a reduction to Pd^0 to become fully catalytically active. Fluorescence imaging experiments later confirmed that the reaction occurred intracellularly as we could follow the release of RhoM in the cytoplasm (Fig. 6c).

Nonetheless, **Pd13** and **Pd14** demonstrated moderate cell survival, whereas Xantphos bearing **Pd2** was found to be highly cytotoxic (Fig. 5b). As a result, the high fluorescence observed was attributed to RhoMA release in the extracellular milieu as the cells died from the toxic effects of these palladium sources. Later, fluorescence imaging experiments confirmed this observation (Fig. 6d). The intracellular fluorescence intensity (calculated by ImageJ and R software) increased at first before gradually decreasing, while the background signal became stronger. This showed that the

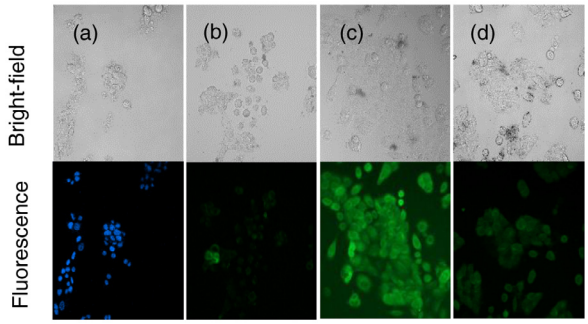

Fig. 6. Fluorescence microscopy imaging of Palladium-induced uncaging of RhoMA inside SiHa cells. (a) Negative control: cells were preincubated with RhoMA (500 µM), TFP (40 µM), and nucleic acid stain (Hoechst 33,342, 1 µg/mL) for 30 min, washed with PBS solution two times; (b) Positive control: cells were preincubated with RhoM (500 µM) and TFP (40 µM) for 30 min, washed with PBS solution two times; Cells were preincubated with RhoMA (500 µM) for 30 min, washed with PBS solution two times, then treated with (c) **Pd1** (20 µM) or (d) **Pd2** (20 µM) and TFP (40 µM) for 28 min.

palladium-catalyzed cleavage reaction occured within the cells before spreading to the extracellular milieu (Fig. S13 and Fig. S14).

3.6. Plausible mechanism for the activation of palladacyclic precatalysts via a Heck-type reaction

In this work, novel aryl palladacyclic complexes containing acetanilide functionalities can perform bioorthogonal Tsuji-Trost deallylation reactions. However, these Pd^{II} palladacycles cannot directly enter the Tsuji-Trost catalytic cycle, without being first reduced to Pd^0. Therefore, we hypothesized that the palladacycles could undergo a Heck-type reaction with the allyl group of the alloc protecting group to initiate a cascade Heck/Tsuji-Trost reaction.

To confirm the reduction of Pd^{II} to Pd^0, we performed a model reaction with Pd1 and allylbenzene in the presence of TEA, which generated a mixture of arylation Heck-type reaction products and palladium-black formation (Scheme 2a). Detection of Heck products by LC-MS supported this hypothesis. Without TEA, no reaction occured when **Pd1** and allylbenzene were mixed under the same conditions (Fig. S9). The proposed catalytic cycle for *in vitro* experiments is illustrated in Scheme 2, where the $Pd^{(0)}L_n$ released after Heck coupling coordinates with NcoumAlloc to form a η^2-allyl-Pd° complex **2**. This complex undergoes oxidative addition to form a η^3-allyl-Pd^{II} intermediate **3**, which releases CO_2 to form η^3-allyl-Pd^{II} **4**. When the nucleophile attacks this intermediate **4**, two scenarios are possible. First, when there is only one equivalent of TEA with **Pd1**, water could act as the nucleophile and react with **4**to form Pd^0L_n and **1a**. Then, **1a,** being more nucleophilic than water, attacks η^3-allyl-Pd^{II} **4** to produce byproduct **1b**, which can also be generated by an intramolecular mechanism involving fast reductive elimination through the intermediate **4** (Scheme 2b, Fig. S10). Second, when TEA is in excess, it becomes the most plausible nucleophile and reacts with η^3-allyl-Pd^{II} **4** to form product **1a** (Scheme 2c, Fig. S10).

This hypothesis was confirmed in LC-MS studies, which revealed that excess TEA was inhibits the generation of byproduct **1b**. However, byproduct 1c was observed when the reaction was carried using 0.1 equivalent **Pd1** and 0.1 equivalent TEA, due to NcoumAlloc acting as a nucleophile to attack η^3-allyl-Pd^{II} 4 (Fig. S11). It is worth noting that these experiments were conducted *in vitro*. However, it is difficult to exclude the possibility of intracellular bio-reductants such as thiols of cofactors or NADH activating the precatalysts in the complex cellular media. Nonetheless, these observations provide a foundation for future investigations into the activation mechanism of the precatalysts in aqueous environments.

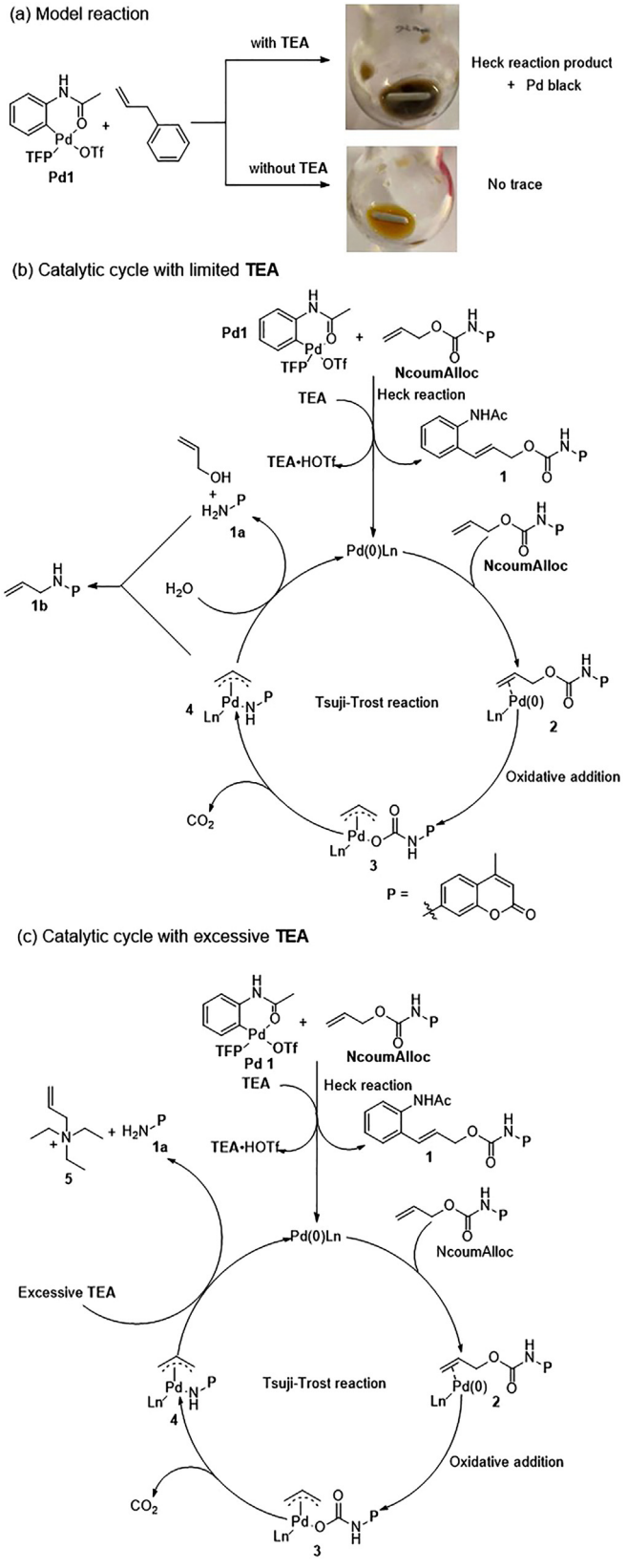

Scheme 2. (a) The Heck model reaction. Reaction conditions: **Pd1** = 30 mM, Allylbenzene = 300 mM, TEA = 300 mM, in CH_3CN, RT, 22 h. (b) Hypothetic Catalytic cycle for the deprotection of NcoumAlloc catalyzed by **Pd1** with limited TEA. Reaction conditions: NcoumAlloc = 320 μM (1 equiv), **Pd1** = 320 μM (1 equiv), TEA = 320 μM (1 equiv), 0.5 ml CH_3CN, RT 3 h. (c) Hypothetic catalytic cycle for the deprotection of NcoumAlloc catalyzed by **Pd1** with an excess of TEA. Reaction conditions: NcoumAlloc = 320 μM (1 equiv), **Pd1**= 320 μM (1 equiv), TEA = 16 mM (50 equiv), 0.5 ml CH_3CN, RT 3 h.

4. Conclusion

In conclusion, we designed and synthesized a library of air- and moisture-stable monoligated aryl palladacyclic complexes with acetanilide functionalities for new applications in bioorthogonal catalytic uncaging of allyloxycarbonyl-protected amines. The results have demonstrated that these complexes might enable fast reaction rates, which is crucial for their potential use in biological systems [37,45]. Notably, **Pd1** displayed a second-order reaction rate of 30 M^{-1} s^{-1} under biologically relevant conditions and efficient activity within mammalian cells. Inspired by the works of Weissleder [26,27] and Koide [39], we demonstrated that the TFP ligand has a major influence on the stability and reactivity of the catalysts under biologically relevant conditions as well as within the cellular cytoplasm. Furthermore, we have demonstrated the potential of a monoallyloxycarbonyl-protected rhodamine 110 (RhoMA) as a reporter for the efficiency of palladium-mediated deallylation reaction, which successfully occured within SiHa cells in an effective OFF/ON mode, without the formation of reaction intermediates. We have also proposed a possible tandem Heck/Tsuji-Trost reaction for the activation-deallylation, which offers a promising starting point for the design of discrete catalytic organometallics as tools in bioorthogonal chemistry.

CRediT authorship contribution statement

Yonghua Tan: Methodology, Data curation, Formal analysis, Investigation, Writing-original draft. Marine Lefèvre: Methodology, Data curation, Formal analysis, Investigation, Writing. François Pierrard, Mathieu Soetens, Maria Shoueiry, Esra Yildiz, Sébastien Ibanez, Kubra Ozkan: Data curation, Investigation. Olivier Feron: Supervision, Methodology, Visualization, Investigation, Writing – review & editing. Raphaël Frédérick: Supervision, Methodology, Visualization, Investigation, Writing –review & editing. Olivier Riant: Supervision, Methodology, Visualization, Investigation, Writing – review & editing.

Declaration of Competing Interest

The authors declare that they have no known competing financial interest or personal relationships that could have appeared to influence the work reported in this paper.

Data availability

Data will be made available on request.

Acknowledgments

We acknowledge the Institute of Condensed Matter and Nanosciences (IMCN) and Louvain Drug Research Institute (LDRI) in UCLouvain, and the Fonds National de la Recherche Scientifique FNRS (MIS grant F.4513.18 for G.B.) for generous funding. Yonghua Tan was supported through a Ph.D. grant from the China Scholarship Council (CSC, 201908320489). The authors also thank Dr. S. Ouk for his generous financial support through the Foundation Louvain allowing the purchase of a solvents purification system.

Supplementary materials

Supplementary material associated with this article can be found, in the online version, at doi:10.1016/j.jorganchem.2023.122743.

References

[1] E.M. Sletten, C.R. Bertozzi, Bioorthogonal chemistry: fishing for selectivity in a sea of functionality, Angew Chem Int Ed Engl 48 (38) (2009) 6974–6998, doi:10.1002/anie.200900942.
[2] S.L. Scinto, D.A. Bilodeau, R. Hincapie, W. Lee, S.S. Nguyen, M. Xu, C.W. Am Ende, M.G. Finn, K. Lang, Q. Lin, J.P. Pezacki, J.A. Prescher, M.S. Robillard, J.M. Fox, Bioorthogonal chemistry, Nat. Rev. Methods. Primers. 1 (2021), doi:10.1038/s43586-021-00028-z.
[3] J.G. Rebelein, T.R. Ward, In vivo catalyzed new-to-nature reactions, Curr Opin Biotechnol 53 (2018) 106–114, doi:10.1016/j.copbio.2017.12.008.
[4] M. Soetens, F. Drouet, O. Riant, (η5-Pentamethylcyclopentadienyl)iridium Complex Catalyzed Imine Reductions Utilizing the Biomimetic 1,4-NAD(P)H Cofactor andN-Benzyl-1,4-dihydronicotinamide as the Hydride-Transfer Agent, ChemCatChem 9 (6) (2017) 929–933, doi:10.1002/cctc.201601307.
[5] C.R. Bertozzi, A decade of bioorthogonal chemistry, Acc. Chem. Res. 44 (9) (2011) 651–653, doi:10.1021/ar200193f.
[6] E. Latocheski, G.M. Dal Forno, T.M. Ferreira, B.L. Oliveira, G.J.L. Bernardes, J.B. Domingos, Mechanistic insights into transition metal-mediated bioorthogonal uncaging reactions, Chem. Soc. Rev. 49 (21) (2020) 7710–7729, doi:10.1039/d0cs00630k.
[7] T. Willemse, K. Van Imp, R.J.M. Goss, H.W.T. Van Vlijmen, W. Schepens, B.U.W. Maes, S. Ballet, Suzuki-Miyaura Diversification of Amino Acids and Dipeptides in Aqueous Media, ChemCatChem 7 (14) (2015) 2055–2070, doi:10.1002/cctc.201500190.
[8] M. Desage-El Murr, Nature is the Cure: engineering Natural Redox Cofactors for Biomimetic and Bioinspired Catalysis, ChemCatChem 12 (1) (2019) 53–62, doi:10.1002/cctc.201901642.
[9] T.S.H. Pfeiffer, U. Schatzschneider, Bioorthogonal oxime ligation of a Mo(CO)4(NeN) CO-releasing molecule (CORM) to a TGF b-binding peptide, J Organomet Chem 734 (2013) 17–24, doi:10.1016/j.jorganchem.2012.09.016.
[10] Y.A. Vessieres, M.J. Wang, G. McGlinchey, Jaouen Multifaceted chemical behaviour of metallocene (M = Fe, Os) quinone methides. Their contribution to biology, Coord Chem Rev 430 (2021) 213658, doi:10.1016/j.ccr.2020.213658.
[11] S.V. Chankeshwara, E. Indrigo, M. Bradley, Palladium-mediated chemistry in living cells, Curr. Opin. Chem. Biol. 21 (2014) 128–135, doi:10.1016/j.cbpa.2014.07.007.
[12] A.D.L.A. Stein, R. Sahin, T.R. Ward, Incorporation of metal-chelating unnatural amino acids into halotag for allylic deamination, J Organomet Chem 962 (2022) 122272, doi:10.1016/j.jorganchem.2022.122272.
[13] M. Martínez-Calvo, J.L. Mascareñas, Organometallic catalysis in biological media and living settings, Coord. Chem. Rev. 359 (2018) 57–79, doi:10.1016/j.ccr.2018.01.011.
[14] Y. Bai, J. Chen, S.C. Zimmerman, Designed transition metal catalysts for intracellular organic synthesis, Chem. Soc. Rev. 47 (5) (2018) 1811–1821, doi:10.1039/c7cs00447h.
[15] J. Miguel-Ávila, M. Tomás-Gamasa, A. Olmos, P.J. Pérez, J.L.J.C.s. Mascareñas, Discrete Cu (I) complexes for azide–alkyne annulations of small molecules inside mammalian cells, Chem.Sci 9 (7) (2018) 1947–1952, doi:10.1039/C7SC04643J.
[16] E.V. Vinogradova, Organometallic chemical biology: an organometallic approach to bioconjugation, Pure Appl. Chem. 89 (11) (2017) 1619–1640, doi:10.1515/pac-2017-0207.
[17] K.C. Nicolaou, P.G. Bulger, D. Sarlah, Palladium-catalyzed cross-coupling reactions in total synthesis, Angew. Chem., Int. Ed. Engl. 44 (29) (2005) 4442–4489, doi:10.1002/anie.200500368.
[18] C.C. Johansson Seechurn, M.O. Kitching, T.J. Colacot, V. Snieckus, Palladium-catalyzed cross-coupling: a historical contextual perspective to the 2010 Nobel Prize, Angew. Chem., Int. Ed. 51 (21) (2012) 5062–5085, doi:10.1002/anie.201107017.
[19] M. Pagliaro, V. Pandarus, R. Ciriminna, F. Béland, P.Demma Carà, Heterogeneous versus homogeneous palladium catalysts for cross-coupling reactions, ChemCatChem 4 (4) (2012) 432–445, doi:10.1002/cctc.201100422.
[20] R.C. Brewster, E. Klemencic, A.G. Jarvis, Palladium in biological media: can the synthetic chemist's most versatile transition metal become a powerful biological tool? J Inorg Biochem 215 (2021) 111317, doi:10.1016/j.jinorgbio.2020.111317.
[21] T. Schlatzer, J. Kriegesmann, H. Schroder, M. Trobe, C. Lembacher-Fadum, S. Santner, A.V. Kravchuk, C.F.W. Becker, R. Breinbauer, Labeling and natural post-translational modification of peptides and proteins via chemoselective Pd-catalyzed prenylation of cysteine, J Am Chem Soc 141 (37) (2019) 14931–14937, doi:10.1021/jacs.9b08279.
[22] R.M. Yusop, A. Unciti-Broceta, E.M. Johansson, R.M. Sanchez-Martin, M. Bradley, Palladium-mediated intracellular chemistry, Nat Chem 3 (3) (2011) 239–243, doi:10.1038/nchem.981.
[23] J. Clavadetscher, E. Indrigo, S.V. Chankeshwara, A. Lilienkampf, M. Bradley, In-Cell Dual Drug Synthesis by Cancer-Targeting Palladium Catalysts, Angew. Chem. Int. Ed. 56 (24) (2017) 6864–6868, doi:10.1002/anie.201702404.
[24] B.Z. Ismaili H, J. Matic, D. Saftic, M. Jukic, L. Glavas-Obrovac, B. Zinic, An efficient synthesis and in vitro cytostatic activity of 5-aminosulfonyl uracil derivatives, Croat. Chem. Acta 92 (2) (2019) 269–277, doi:10.5562/cca3567.
[25] H.Y. Che, H.Y. Guo, X.W. Si, Q.Y. You, W.Y. Lou, PP121, a dual inhibitor of tyrosine and phosphoinositide kinases, inhibits anaplastic thyroid carcinoma cell proliferation and migration, Tumour Biol 35 (9) (2014) 8659–8664, doi:10.1007/s13277-014-2118-3.

[26] M.A. Miller, B. Askevold, H. Mikula, R.H. Kohler, D. Pirovich, R. Weissleder, Nano-palladium is a cellular catalyst for in vivo chemistry, Nat. Commun. 8 (2017) 15906, doi:10.1038/ncomms15906.
[27] J.T. Weiss, J.C. Dawson, K.G. Macleod, W. Rybski, C. Fraser, C. Torres-Sánchez, E.E. Patton, M. Bradley, N.O. Carragher, A. Unciti-Broceta, Extracellular palladium-catalysed dealkylation of 5-fluoro-1-propargyl-uracil as a bioorthogonally activated prodrug approach, Nat. Commun. 5 (1) (2014) 3277, doi:10.1038/ncomms4277.
[28] J. Wang, B. Cheng, J. Li, Z.Y. Zhang, W.Y. Hong, X. Chen, P.R. Chen, Chemical remodeling of cell-surface sialic acids through a palladium-triggered bioorthogonal elimination reaction, Angew. Chem. Int. Ed. 127 (18) (2015) 5454–5458, doi:10.1002/ange.201409145.
[29] M. Martinez-Calvo, J.R. Couceiro, P. Destito, J. Rodriguez, J. Mosquera, J.L. Mascarenas, Intracellular deprotection reactions mediated by palladium complexes equipped with designed phosphine ligands, ACS Catal 8 (7) (2018) 6055–6061, doi:10.1021/acscatal.8b01606.
[30] J. Li, J. Yu, J. Zhao, J. Wang, S. Zheng, S. Lin, L. Chen, M. Yang, S. Jia, X. Zhang, P.R. Chen, Palladium-triggered deprotection chemistry for protein activation in living cells, Nat. Chem. 6 (4) (2014) 352–361, doi:10.1038/nchem.1887.
[31] J. Wang, S. Zheng, Y. Liu, Z. Zhang, Z. Lin, J. Li, G. Zhang, X. Wang, J. Li, P.R. Chen, Palladium-Triggered Chemical Rescue of Intracellular Proteins via Genetically Encoded Allene-Caged Tyrosine, J. Am. Chem. Soc. 138 (46) (2016) 15118–15121, doi:10.1021/jacs.6b08933.
[32] C.V. Soraya Learte-Aymamí, Alejandro Gutiérrez-González, José L. Mascareñas, Intracellular reactions promoted by bis-histidine miniproteins stapled with Pd(II) complexes, Angew. Chem. Int. Ed. 59 (23) (2020) 9149–9154, doi:10.1002/anie.202002032.
[33] J.C. Eugenio Indrigo, Sunay V. Chankeshwara, Alicia Megia-Fernandez, Annamaria Lilienkampf, Mark Bradley, Intracellular delivery of a catalytic organometallic complex, Chem. Commun. 53 (2017) 6712–6715, doi:10.1039/C7CC02988H.
[34] C.S. Wei, G.H. Davies, O. Soltani, J. Albrecht, Q. Gao, C. Pathirana, Y. Hsiao, S. Tummala, M.D. Eastgate, The impact of palladium(II) reduction pathways on the structure and activity of palladium(0) catalysts, Angew. Chem., Int. Ed. 52 (22) (2013) 5822–5826, doi:10.1002/anie.201210252.
[35] J. Konc, V. Sabatino, E. Jimenez-Moreno, E. Latocheski, L.R. Perez, J. Day, J.B. Domingos, G.J.L. Bernardes, Controlled In-Cell Generation of Active Palladium(0) Species for Bioorthogonal Decaging, Angew. Chem. Int. Ed. 61 (8) (2022) e202113519, doi:10.1002/anie.202113519.
[36] C. Zhang, K. Ogawa, S. Tu, C. Zu, J. Ringer, C. Derstine, H. Do, P.P. Fontaine, J. Klosin, Highly Active Monoligated Arylpalladacyles for Cross-Coupling Reactions, Org. Pro. Res. Dev. 23 (10) (2019) 2181–2190, doi:10.1021/acs.oprd.9b00234.
[37] T. Völker, E. Meggers, Chemical activation in blood serum and human cell culture: improved ruthenium complex for catalytic uncaging of alloc-protected amines, ChemBioChem 18 (12) (2017) 1083–1086, doi:10.1002/cbic.201700168.
[38] A. DeAngelis, P.G. Gildner, R. Chow, T.J. Colacot, Generating active "L-Pd (0)" via neutral or cationic π-allylpalladium complexes featuring biaryl/bipyrazolylphosphines: synthetic, mechanistic, and structure–activity studies in challenging cross-coupling reactions, J. Org. Chem. 80 (13) (2015) 6794–6813, doi:10.1021/acs.joc.5b01005.
[39] A.L. Garner, F. Song, K. Koide, Enhancement of a catalysis-based fluorometric detection method for palladium through rational fine-tuning of the palladium species, J. Am. Chem. Soc. 131 (14) (2009) 5163–5171, doi:10.1021/ja808385a.
[40] J.A. Menges, A. Grandjean, A. Clasen, G. Jung, Kinetics of Palladium(0)-Allyl Interactions in the Tsuji-Trost Reaction, derived from Single-Molecule Fluorescence Microscopy, ChemCatChem 12 (9) (2020) 2630–2637, doi:10.1002/cctc.202000032.
[41] J. Xu, H. Li, X. Wang, J. Huang, S. Li, C. Liu, R. Dong, G. Zhu, C. Duan, F.J.E.J.o.M.C. Jiang, Discovery of coumarin derivatives as potent and selective cyclin-dependent kinase 9 (CDK9) inhibitors with high antitumour activity, Eur. J. Med. Chem. 200 (2020) 112424, doi:10.1016/j.ejmech.2020.112424.
[42] Y. Liu, P. Turunen, B.F. de Waal, K.G. Blank, A.E. Rowan, A.R. Palmans, E.W. Meijer, Catalytic single-chain polymeric nanoparticles at work: from ensemble towards single-particle kinetics, Mol.Syst.Des.Eng 3 (4) (2018) 609–618, doi:10.1039/C8ME00017D.
[43] L. Brisson, P. Banski, M. Sboarina, C. Dethier, P. Danhier, M.J. Fontenille, V.F. Van Hee, T. Vazeille, M. Tardy, J. Falces, C. Bouzin, P.E. Porporato, R. Frederick, C. Michiels, T. Copetti, P. Sonveaux, Lactate Dehydrogenase B controls lysosome activity and autophagy in cancer, Cancer Cell 30 (3) (2016) 418–431, doi:10.1016/j.ccell.2016.08.005.
[44] M.A. Miller, B. Askevold, H. Mikula, R.H. Kohler, D. Pirovich, R. Weissleder, Nano-palladium is a cellular catalyst for in vivo chemistry, Nat. Commun. 8 (1) (2017) 15906, doi:10.1038/ncomms15906.
[45] T. Volker, E. Meggers, Chemical Activation in Blood Serum and Human Cell Culture: improved Ruthenium Complex for Catalytic Uncaging of Alloc-Protected Amines, Chembiochem 18 (12) (2017) 1083–1086, doi:10.1002/cbic.201700168.